Title

- Full title: PRR adjuvants restrain high stability peptides presentation on APCs
- Running title: Adjuvants restrain stability-peptides presentation

Authors

Bin Li*†[1], Jin Zhang†[1], Taojun He[1], Hanmei Yuan[1], Hui Wu[1], Peng Wang*[2], Chao Wu*[1].

Affiliations

[1]Department of Laboratory Medicine, The Eighth Affiliated Hospital of Sun Yat-sen University, Shenzhen, P.R. China.

[2]Department of Orthopedics, The Eighth Affiliated Hospital of Sun Yat-sen University, Shenzhen, P.R. China.

*Corresponding author. Email: Chao Wu (wuch57@mail.sysu.edu.cn), Bin Li (libin2005017@163.com) and Peng Wang (wangp57@mail.sysu.edu.cn)

† These authors share the co-first author.

Abstract

Adjuvants can affect the function of APCs and boost the adaptive immune responses post vaccination. However, whether adjuvants modulate the specificity of immune responses, especially the specificity of immunodominant epitope responses, and the mechanisms of adjuvants regulating antigen processing and presentation remain poorly defined. Here, using overlapping synthetic peptides, we screened the dominant epitopes of Th1 responses in mice post vaccination with different adjuvants and found that adjuvants altered antigen-specific $CD4^+$ T cell immunodominant epitope hierarchy. MHC-II immunopeptidome demonstrates that peptide repertoires presented by APCs are altered by adjuvants

significantly. Unexpectedly, no novel peptide presentation was detected post adjuvants treatment, on the contrary, peptides with high binding stability for MHC-II presented in the control group were missing post adjuvant stimulation, especially in the MPLA and CpG group. The low stability peptide presented in adjuvant groups elicited robust T cell responses effectively and formed immune memory. Taken together, our results suggest that adjuvants (MPLA and CpG) restrain high stability peptides presentation instead of revealing cryptic epitopes, which may alter the specificity of the $CD4^+$ T-cell dominant epitope responses. This capacity of adjuvants to modify pMHC stability and antigen-specific T cell immunodominant epitope responses has fundamental implications for the selection of suitable adjuvants in the vaccine design process and the development of epitope vaccines.

Keywords: Vaccine; Adjuvants; Immunization; T cell

Introduction

Adjuvants are an important composition of vaccines, which enhance or prolong the immune responses to co-administered antigens post vaccination. Most commonly used adjuvants stimulate Ab responses relying on B cells.(*1, 2*) The priming of B cells and the forming of B cell memory are dependent on the cognate help of antigen-specific T cells. Besides, T cells have direct effector functions against pathogen infection. Thus, antigen-specific T cells play a vital role in shaping immune responses in the setting of vaccination. However, the mechanisms of adjuvants regulating the specificity of antigen-specific T cell responses remain poorly resolved.

Antigen-specific T cell responses mainly focus on several peptides derived from antigen amino acids called immunodominant epitopes.(*3*) Although specific T cell responses were provoked by the same antigen, their response epitopes may be different, which leads to diverse effects. Peptides presented by APCs (antigen presenting cells) provide the first major signal for the priming of T cells and determine the specificity. Although it has been confirmed that adjuvants can activate APCs, and increase the expression of costimulatory molecules of APCs,(*4*) it has not been demonstrated how adjuvants affect the peptide repertoires presented by APCs or modulate epitope-specific T cell responses.

Helicobacter pylori (*H. pylori/* Hp) infects more than half of the world's population and causes chronic gastritis, peptic ulcers, gastric mucosa-associated lymphoid tissue lymphoma (MALT) and gastric cancer.(*5, 6*) Studies in human and mouse models showed that Th1 response provides more important protection against *H. pylori* than a humoral immune response. Unfortunately, no effective vaccines driving T cell responses have been developed so far.(*7*) *H. pylori* provides an ideal experimental model to determine the mechanisms of adjuvants regulating T cell responses.

Studies of the widely used adjuvant have found that some pattern-recognition receptor (PRR) ligand adjuvants can induce strong T cell response.(*8*, *9*) PRR ligand adjuvants targeting PRRs on the surface of innate immune cells such as macrophages and dendritic cells, promote cytokines secretion and upregulate co-stimulatory molecule expressions.(*10*) Typical PRR adjuvants include MPLA, CpG and MDP, which have been confirmed to induce effective T cell responses and have been successfully used in many vaccines such as HPV, HSV, and COVID-19 vaccines.(*11-13*) However, their impact on antigen processing and presentation in APCs, and immunodominant epitope responses are not known.

In this study, using MPLA, CpG and MDP adjuvants and *H. pylori* antigens, we demonstrate that immunodominant epitopes recognized by antigen specific T cells are altered by adjuvants. Furthermore, we show that adjuvants, MPLA and CpG especially, modulate the peptide repertoires presented on the surface of APCs. Surprisingly, instead of revealing cryptic epitopes or presenting high-stability peptides, peptides with high binding stability for MHC-II are restained and low-stability peptides were presented by APCs post adjuvants treatment. And, the low stability peptide presented in adjuvant groups elicits T cell response effectively. Thus, altering pMHCII stability presented on APCs provides a fundamentally new mechanism for PRR adjuvants regulating adaptive immunity. The implications of this observation are discussed.

Results

Immunodominant T cell epitopes hierarchy varies in vaccinated mice with different adjuvants

To determine the influences of adjuvants on the specificity of immune responses, BALB/c mice were vaccinated with antigen UreB, one effective antigen for the *H. pylori* vaccine, combined with adjuvants CpG, MDP and MPLA respectively. Then, antigen specific T cells from immunized mice were expanded and their IFN-γ responses to 93 individual UreB overlapping 18mer peptides were screened using flow cytometry. 18mer peptides U313-330 and U403-426 were primarily recognized in the CpG group. T cells from the MDP group have dominant responses to U409-426 and U481-498. T cells from the MPLA group primarily recognized U313-U330 and U505-522, whereas U481-U504 was the dominant region in the no adjuvant group (Figure 1). These data indicated that immunodominant epitopes responded by antigen-specific T cells varied in different adjuvant vaccination groups.

Profiling MHC-II peptides in adjuvants-treated APCs

Considering that T cell repertoires are the same in naive mice, we speculate that dominant epitope variations in different adjuvant vaccination groups result from the alteration of peptide presentation of APCs. To interrogate the repertoire of MHC-II peptides presented by APCs, antigens from *H. pylori* ultrasonic supernatant were used to pulse H-2^d A20 cells combined with adjuvants CpG, MDP and MPLA respectively. Then, MHC-II-peptide complexes were immunoprecipitated. The bound peptides were eluted and identified by liquid chromatography-tandem MS (LC-MS/MS) (Figure 2A). The whole proteomes of protein-pulsed A20 cells were also analyzed by LC-MS/MS to examine the effect of adjuvants on extracellular antigen phagocytosis and gene expression associated with antigen processing and presentation.

A total of 4074 peptides were identified, 3408 peptides in the PBS group, 3257 peptides in the MDP group, 3227 peptides in the MPLA group, and 3330 peptides in the CpG group,

respectively. As expected, the number and length distribution of peptides were not influenced by adjuvants (Figure 2B and 2C). The majority of identified peptides were 16 mers. Next, the binding motifs of all peptides identified in different groups were analyzed (Figure 2D). No obvious differences following adjuvant treatment were identified. The binding motifs of peptides per individual MHC-II allele, H2-IA and H2-IE were also analyzed (Figure S1). No major differences were detected. The observed amino acids at the main anchor location are consistent with the expected binding motifs. Binding affinity data predicted using NetMHCIIpan showed that most MS-detected peptides were indeed predicted to bind with MHC-II alleles (%rank <10) and assigned to the H2-IA allele generally (Figure 2E; Figure S1). These results indicate that adjuvants were not able to affect MHC-II binding characteristics.

We also chose another H-2^d cell J774A.1, a macrophage cell line, for immunopeptidome in this study. Unfortunately, MHC-II molecular expression on J774A.1 was much lower than that on A20 cells. Even 5 times J774A.1 cells more than A20 cells were used, no enough peptides were identified by LC-MS/MS (Figure S2). Thus, A20 cells were used in our following experiments.

Adjuvants affected the presentation of exogenous peptides exclusively

Next, we examined the exogenous peptides across the *H. pylori* genome from MHC-II immunopeptidome. Surprisingly, *H. pylori* contains more than 3,000 proteins, but only no more than 30 proteins were detected from MHC-II immunopeptidome (Figure 3A). To test if the MHC-IP (MHC-immunoprecipitation) identified proteins have higher levels of expression in bacteria, we ranked the individual *H. pylori* proteins according to their abundance. The abundance of MHC-IP identified proteins in whole *H. pylori* proteome MS data was analyzed, and we found that the abundance of these proteins is similar to the

other bacterial proteins (Figure 3B). Then, we wondered whether MHC-IP proteins harbor more peptides compatible with the MHC-II, so we compared the ratio between the number of peptides that are predicted to bind MHC-II alleles and the total number of 13- to 17-mers. Obviously, MHC-IP proteins have more presentable peptides than most other bacterial proteins (Figure 3C).

Through analyzing the host and exogenous MHC-II peptides presented in different adjuvant groups, we found that 82.4% of host MHC-II peptides were presented in all the groups, however, only 34.4% of exogenous MHC-II peptides were conserved post adjuvants treatment (Figure 3D; Figure S3). These data indicated that adjuvants affected the presentation of exogenous peptides particularly. Many exogenous peptides were missing post adjuvants MPLA or CpG treatment. However, no changes of the number of peptides from the host were detected (Figure 3E). The above data indicate that the repertoires of exogenous peptides presented by APCs are affected exclusively by adjuvants and a smaller number of peptides are presented.

Adjuvants may affect antigen processing but not phagocytosis

To test if the changes of exogenous peptide presentation among adjuvant groups could be explained by differences in antigen phagocytosis, we examined the whole proteome data. We found a strong correlation of abundance of bacterial proteins between different adjuvants treated groups (Figure 4A). We further compared the abundance of bacterial proteins in the proteome and MHC-II immunopeptidome. We found that the abundance of bacterial proteins presented in the immunopeptidome changed significantly among adjuvant groups, and even no peptides of several bacterial antigens were detected in some groups. However, only several proteins altered abundances in the proteome (Figure 4B).

These results suggested that changes of exogenous peptide presentation among adjuvant groups could not be explained by antigen phagocytosis.

To further investigate how adjuvants affect the bacterial antigens to be processed and presented, we ranked the individual proteins and MHC-II peptides derived from bacteria according to their abundance in comparison with those from the host. The overall abundance of bacterial proteins in the APCs proteome was low (Figure S4A). And, individual bacterial proteins expressions were below most of the host proteins both in PBS and adjuvants groups (Figure 5A). In contrast to the low abundance of bacterial proteins, the intensities of their MHC-II peptides are similar to peptides from the host in the PBS group according to the immunopeptidome data (Figure 5B), indicating that bacterial peptides are presented preferentially. However, in the MPLA and CpG groups, the intensities of bacterial MHC-II peptides in immunopeptidome were much lower than those from the host (Figure 5B). These results indicate that adjuvant MPLA and CpG restrain bacterial peptide presentation.

Then, we analyzed the whole proteome data to determine whether the proteins involved in antigen presentation and processing were altered. We found that proteins involved in antigen processing, peptidase function, ubiquitination pathway and interferon (IFN) signaling were altered post adjuvants treatment, especially in MPLA and CpG groups (Figure 5C; Figure S4B and S4C). These data suggest that adjuvants MPLA and CpG may affect the antigen processing of APCs, resulting in fewer peptides presentation.

High-stability epitopes were deficient in adjuvants MPLA and CpG groups

To further characterize adjuvant effects on peptide presentation, the MHC binding affinity of the peptides presented in adjuvants groups and that of the peptides deficient post adjuvants stimulation were analyzed using the IEDB website. The IC50 values of

presented peptides assigned to H2-IA and H2-IE alleles were much higher than deficient peptides, which indicated that the peptides presented in adjuvant groups have lower binding stability for MHC-II (Figure 6A). At cutoffs of predicted percentile rank <2 (Strong Binders) or <10 (Weak Binders), similar results were detected (Figure S5). Furthermore, we found that the presented peptides in adjuvant goups were mainly derived from protein tuf, recA, etc., and the deficient peptides were mainly derived from protein ureA, hopZ, etc. (Figure 6B). To validate the amino acid sequences of MS-detected peptides and the binding stability of peptides, 10 peptides derived from Top4 presented and deficient proteins shown in Figure 6B were synthesized (Figure 6C). The tandem mass spectra of synthetic peptides and the experimental spectra were compared, and high correlations between fragment ions and retention times were observed (Figure 6D). Then, we performed the MHC-II competition binding assay to detect the binding stability of 10 synthetic peptides in the presence of one competing MHC-II ligand. We confirmed that peptides that were missing in adjuvant groups have better binding stability for MHC-II molecules in comparison with peptides presented in adjuvant groups (Figure 6E). These data indicate that epitopes with high binding stability are deficient post adjuvants MPLA and CpG treatment.

Low-stability peptide presented in adjuvant groups induce robust T cell responses effectively

To evaluate if the low stability peptides presented in adjuvant groups could induce T cell responses or not, mice were immunized with a pool of 10 synthetic peptides. Cell responses to individual peptides were detected using IFN-γ Elispot assay on day 10 (effective phase) and day 28 (memory phase) post-immunization (Figure 7A). We found positive responses to low stability peptides recA #23 (AFIDAEHALDVHYAKR) and NCTC11637-00693 #38 (IHSQVEANTQAQEGLR), as well as to high stability peptides

ureA #2 (ASMIHEVGIEAMFPDGTK), ureA #3(YVEAVALISAHIMEEAR) and hopZ #53(KMLELANQIKTNLSAIPQ) on day 10 (Figure 7B). On day 28, the response to the low stability peptide recA #23 (AFIDAEHALDVHYAKR) was not weaker than the other peptides (Figure 7C). It was reported that peptides with low stability for MHC-II skew T-cell repertoires towards high-affinity clonotypes which had better responses against pathogen infection.(14, 15) To assess the functional avidities of T cell responses induced by the low stability peptide presented in adjuvant groups, peptide-specific $CD4^+$ T cells were expanded *in vitro*. And, the magnitude of IFN-γ responses was detected by ICS using flow cytometry on stimulation with a set of titrated peptides. We found that low stability peptide recA #23 induced more robust $CD4^+$ T cell responses at lower peptide concentrations (Figure 7D). These data suggest that low stability peptide presented in adjuvant groups could induce robust $CD4^+$ T cell responses effectively.

Discussion

We have demonstrated that adjuvants alter the specificity of dominant Th1 epitope responses post-vaccination. Using LC-MS/MS based MHC-II immunopeptidome, peptides of *H. pylori* antigens presented by APCs under the stimulation of different adjuvants were analyzed. The motifs of presented peptides binding to MHC-II are consistent generally following the stimulation of adjuvants. However, the exogenous peptide repertoires presented by APCs change obviously. Low stability peptides and high stability peptides were presented by APCs in the control group, however, fewer peptides were detected in adjuvant groups, and peptides with high binding stability for MHC-II presented in control group were missing post adjuvant stimulation, especially in the CpG group. The low stability peptide presented in adjuvant groups have good immunoreactivity inducing effector and memory immune responses effectively. Thus, our data suggest that adjuvants

can restain pMHCII stability presented on APCs to regulate dominant epitope-specific T cell responses.

The protective effects of vaccines depend on the immune responses induced post vaccination. For prophylactic vaccines, adaptive immune responses are important which are restricted to a limited number of epitopes. However, not all epitope-specific responses are protective. Some epitope-induced immune responses exacerbate inflammation and autoimmune diseases.(*16-18*) Some epitopes induce the expansion of Tregs and relieve inflammation.(*19*) Thus, the alteration of dominant epitope responses will directly affect vaccine effectiveness. Maeda *et al.* characterized the modulation of adjuvants LT and LTB on antibody responses to a coadministered antigen, EDIII. They showed that LT and LTB adjuvanted specific antibodies displayed distinct linear epitope-binding patterns and fewer peptides were recognized compared with the non-adjuvanted or alum-adjuvanted group.(*20*) However, Borriello *et al.* showed that mannans formulated with alum as an adjuvant broaden epitopes responses of anti-Spike neutralizing antibodies.(*21*) Chung *et al.* reported that ISCOMATRIX™ adjuvant promotes HA1 antibodies against large conformational epitopes spanning the receptor binding domain, while antibodies targeting the C-terminus of the HA1 domain are generated in the unadjuvanted group. However, the numbers of recognized epitopes do not change among groups.(*22*) Although the capacity of adjuvants to modulate the epitope specificity of antibodies has been described, the effects of adjuvants in the modulation of T cell epitope specificity remain unclear.

Lo-Man R *et al.* reported that *Salmonella enterica* expressing MalE protein induced new $CD4^+$ T cell responses to peptides that were silent in purified Ag with adjuvant CFA administration group.(*23*) Andersen e*t al.* showed that adenovirus vector expressing Ag85B/ESAT-6 fusion proteins induced $CD8^+$ T cell response against ESAT-6 epitope, while $CD4^+$ T-cell response to epitope located in Ag85B was detected in the liposomal

adjuvanted group.(*24*) These researches suggest that specific T cell responses are not constant, and antigen delivery formulation can affect the specificity of $CD4^+$ T cell responses. In this study, using a series of synthesized overlapping peptides, we reveal that adjuvants modulate the hierarchy of epitope-specific Th1 responses post vaccination.

Successful priming of epitope-specific T cell requires T-cell receptor (TCR) recognition of peptide-MHC complex (pMHC) on the surface of APCs. Adjuvants have been reported to have the capacity to activate APCs and enhance costimulatory signals.(*25, 26*) However, whether adjuvants can regulate the presentation of pMHC on APCs cell surface remains lacking direct evidence. In this study, using LC-MS/ MS-based immunopeptidome, we confirm that adjuvants affect peptide repertoires presented by MHC-II molecules of APCs, and fewer peptides are presented by APCs post MPLA and CpG stimulation. A narrow peptide repertoire has been reported to increase the possibility of T cell priming and improve the specificity of T cell responses.(*27*) Thus, we speculate that adjuvants MPLA and CpG may enhance vaccine-induced immune response by restricting epitope diversity presentation of APCs rather than inducing more cryptic epitope presentation. Furthermore, we find that peptides with high binding stability for MHC-II are restained and low stability peptides are presented on APCs post MPLA and CpG adjuvants treatment. Peptides with low stability for MHC-II have been confirmed to skew antigen-specific T cell repertoires towards high TCR affinity clonotypes.(*14*) Our data explain Baumgartner and colleagues' finding that MPLA and CpG adjuvants induce high TCR affinity antigen-specific T cell clonotype responses.(*28*) T cell clonotypes with higher TCR affinity have better abilities against pathogen infection and tumor.(*15, 29, 30*) In this study, we also observed robust T cell responses induced by the peptide with low stability through the Titration assay (Figure 7D), although no single T cell clonotype was used.

APCs subtypes differ in the expression of endolysosomal proteases and DO/ DM molecules(*31-33*), and exhibit different abilities to process Ag and present peptides.(*34, 35*) Kanellopoulos *et al.* reported that DCs focused HEL-specific $CD4^+$ T-cell responses against an I-E^d-restricted peptide HEL103-117, while B cells presented an additional I-A^d-restricted peptide HEL7-31.(*36*) Max Schnurr and colleagues had shown that $CD1c^+$ blood DCs and MoDCs were capable of presenting peptides of antigen NY-ESO-1 on both MHC I and MHC II, while pDCs were limited to MHC II presentation.(*37*) In this study, antigen UreB adjuvanted different adjuvants induced antigen-specific $CD4^+$ T cell responses *in vivo* post-vaccination, whereas no peptides of UreB presented by A20 cells were detected *in vitro* using LC-MS/ MS. One reason may be differences in the cell types of APCs involved, with many APCs subtypes involved *in vivo*, especially DCs, but only the B cell line (A20) used *in vitro*. Another reason may be that the UreB peptide abundance is below the detection limit of LC-MS/MS *in vitro*.

Pathogen proteins with high abundance are often preferred as candidate antigens for vaccine design. However, the amounts of pathogen antigens are not consistent with that of antigens which are phagocytized and presented by APCs. Shira Weingarten-Gabbay and colleagues found that nucleocapsid protein (N) is the most abundant viral protein in SARS-CoV-2 infected A549 and HEK293T cells, but only one HLA-I peptide from N is presented.(*38*) Thus, antigens with high expression might be less presented than expected, and induce poor T-cell responses. We found that the proteins harboring more peptides compatible with the MHC binding motifs were more likely to be presented (Figure 3C). Screening the dominant epitopes from all proteins of pathogens is meaningful for vaccine design. This is the advantage of immunopeptidomes based on LC-MS/ MS. Several epitopes detected in this study with good immunogenicity may be used as candidates for epitope vaccine development.

Taken together, our work uncovers that adjuvants influence the pMHC stability presented on APCs and change the specificity of epitope responses. In the process of adjuvant selection for vaccines, it is necessary to consider not only adjuvants' effect on the strength of immune responses, but also that on the specificity of the responses, especially for PRR ligand adjuvants, which mainly induce Th1 or CTL biased responses.

Limitations of the study

First, the peptides screened *in vitro* using cell lines cannot reflect the situation *in vivo*. The epitope presentation of APCs can be affected by APCs subtypes and inflammatory cytokines at the inoculation site(*39*), which are difficult to simulate and reproduce *in vitro*. Second, peptide abundance below the limit of detection may be missed using LC-MS/MS based assays, which may cause false negatives. The possibility of these peptides inducing immune responses cannot be ruled out. Third, compared with mouse MHC molecules, human MHC molecules are much more complex. Whether the research's conclusions can be generalized to the human population still needs further research.

Materials and Methods

Synthetic Peptides, antibodies and other reagents

18mer peptides overlapping by 12 amino acids derived from antigen UreB were synthesized and purified (purity >90%) by ChinaPeptides (Shanghai, China). All peptides were dissolved in dimethyl sulfoxide (Sigma-Aldrich, MO, USA) and stored at -80°C. For information about antibodies and other reagents, see Supplementary Table 1.

Cell culture

Mouse A20 cell (H-2^d, B-cell lymphoma cell line) and mouse J774A.1 cell (H-2^d, monocyte/ macrophage cell line) were obtained from the American Tissue Culture Collection (ATCC, VA, USA). A20 cells were cultured in RPMI 1640 medium (Gibco) containing 10% fetal bovine serum (Biological Industries, Kibbutz Beit Haemek, Israel), 1% L-Glutamine (Gibco) and 1% penicillin/streptomycin (Gibco). J774A.1 cells were maintained in DMED medium (Gibco) supplemented with 10% fetal bovine serum, 1% L-Glutamine and 1% penicillin/streptomycin. All these cell lines were maintained at 37 °C in a humidified incubator with 5% CO_2.

Mice immunization and specific T cell bulk culture

This study was approved by the Animal Ethics Review Committee of the Eighth Affiliated Hospital of Sun Yat-sen University.

Six- to eight-week-old SPF female BALB/c mice were immunized subcutaneously with 100 μg of recombinant *H pylori* UreB (rUreB, purity >95%) emulsified in adjuvants CpG (20 μg/ mouse), MDP (30 μg/ mouse) and MPLA (10 μg/ mouse) respectively. Mice immunized with the same antigen without adjuvants following the same procedure were used as controls. 10 days later, mice were euthanized and spleens were harvested. Antigen-specific T cells were expanded *in vitro* as described previously.(*40*) Briefly, lymphocytes from spleens were isolated using a Ficoll-Hypaque (Dakewe, Shanghai, China) gradient and pulsed with 0.5 μM rUreB protein in the presence of 5 U/ml rmIL-2 (PeproTech, NJ, USA). Cells were cultured in "RF-10" medium consisting of RPMI 1640 (Gibco, CA, USA) supplemented with 10% fetal calf serum (Gibco), 1% L-Glutamine (Gibco), 1× 2-mercaptoethanol (Gibco), and antibiotics (100 U/mL penicillin/ streptomycin, Gibco) *in*

vitro. On day 5, live cells were collected using a Ficoll-Hypaque gradient and cultured in a complete medium containing 20 U/ml rmIL-2. Half of the medium was replaced when required.

Flow cytometry

Bulk cultured T cells were stimulated with 5 μM peptides for 5hr in the presence of brefeldin A (Biolegend). The cells were collected and stained with specific antibodies against surface markers, then, intracellular cytokine staining was performed after fixation. Cells were acquired using an LSRFortessa Flow Cytometer (BD Biosciences, CA, USA) or a Navios Flow Cytometer (Beckman Coulter, FL, USA). Data were analyzed using FlowJo software (Tree Star, CA, USA).

Preparation of *H. pylori* lysates

The *H. pylori* strain NCTC 11637 (ATCC) was used in this study. The *H. pylori* strain was cultured on brain-heart infusion plates with 10% rabbit blood (Sbjbio, Nanjing, China) under 37°C microaerophilic conditions. Then, *H. pylori* was amplified in Brucella broth with 5% fetal bovine serum（BI） under gentle shaking at 37°C microaerophilic conditions for 24hr. Bacterias were collected, washed and resuspended in PBS (Gibco) for lysis using an Ultrasonic dismembrator (Biosafer, Nanjing, China). The lysates were centrifuged at 4°C, 12000 g for 20 min. The supernatant was stored at -80°C for subsequent experiments.

Immunoprecipitation of MHC-II complexes

A20 cells were abundantly expanded in T_{75} cell culture flasks (Corning, NY, USA). The expanded cells were pulsed with *H. pylori* lysates in combination with adjuvants MPLA, MDP or CPG respectively for 12 hr. Then, A20 cells were collected and washed twice with sterile PBS. These cells were divided into two fractions. one fraction, about 10^7 cells, were used for whole-proteome analysis. The rest 10^8 cells were lysed in cold lysis buffer (1.0 % w/v CHAPS, Protease Inhibitor Tablet and PMSF) for immunoprecipitation of MHC-II complexes. The cell lysates were centrifuged at 18,000 g for 20 min. The supernatant (containing the MHC-peptides complexes) was transferred into a new 1.5 ml Eppendorf tube (Corning) containing a mixture of Sepharose CNBr-activated beads (Cytivia, Utah, USA) and 2 mg of Anti-Mouse H2-IA^d/IE^d (M5/114) antibody (BioXcell, NH, USA). The immune complexes were captured on the beads by incubating on a rotor at 4°C for 18 hr. Sequentially, the immune complexes were transferred into a polypropylene column (Bio-Rad Laboratories, CA, USA), and washed with 10 ml buffer A (150 mM NaCl, 20 mM Tris, pH 8.0), 10 ml buffer B (400 mM NaCl, 20 mM Tris, pH 8.0), 10 ml buffer A and 10 ml buffer C (Tris 20 mM, pH 8.0). The MHC-II-peptide complexes were eluted with 300 µl 10% glacial acetic acid (Macklin, Shanghai, China) three times. The eluate was stored at -80°C until mass-spectrometry analysis was performed.

MHC-II peptidome LC-MS/MS data generation

MHC peptides were eluted and desalted from beads as described previously.(*41*) The lyophilized peptides were resuspended in ddH_2O containing 0.1% formic acid, and 2 µl aliquots of which were loaded into a nanoViper C18 (Acclaim PepMap 100, 75 µm×2 cm) trap column. The online Chromatography separation was performed on the Easy nLC 1200 system (Thermo Fisher, MA, USA). The trapping and desalting procedures were carried out with a volume of 20 µl 100% solvent A (0.1% formic acid). Then, an elution gradient of 5% -38% solvent B (80% acetonitrile, 0.1% formic acid) in 60 min was used

on an analytical column (Acclaim PepMap RSLC, 75 μm × 25 cm C18-2 μm 100Å). DDA (data-dependent acquisition) mass spectrum techniques were used to acquire tandem MS data on a ThermoFisher Q Exactive mass spectrometer (Thermo Fisher) fitted with a Nano Flex ion source. Data was acquired using an ion spray voltage of 1.9kV, and an interface heater temperature of 275°C. For a full mass spectrometry survey scan, the target value was 3×10^6 and the scan ranged from 350 to 2,000 m/z at a resolution of 70,000 and a maximum injection time of 100 ms. For the MS2 scan, only spectra with a charge state of 2-5 were selected for fragmentation by higher-energy collision dissociation with a normalized collision energy of 28. The MS2 spectra were acquired in the ion trap in rapid mode with an AGC target of 8,000 and a maximum injection time of 50ms. Dynamic exclusion was set for 25s.

Whole proteome LC-MS/MS data generation

Aliquots of protein were mixed with 200 μl of 8M urea in Nanosep Centrifugal Devices (PALL). The device was centrifuged at 12,000 g at 20°C for 20 min. All following centrifugation steps were performed applying the same conditions allowing maximal concentration. Then, 200 μl of 8 M urea solution with 10 mM DTT was added, and the reduction reaction was kept for 2 hr at 37°C. The solution was removed by centrifugation, and 200 μl 8M urea solution with 50 mM iodoacetamide (IAA) was added. The sample was incubated in the dark for 15 min at room temperature. The ultra-fraction tube was washed with 200 μl of 8M urea three times and 200 μl of 25 mM ammonium bicarbonate three times by centrifugation at 12,000 g for 20 min at room temperature. Then, 100 μl of 25 mM ammonium bicarbonate containing 0.01 μg/μl trypsin was added to each filter tube. The tubes were incubated at 37 °C for 12 hr. The filter tubes were washed twice with 100 μl of 25 mM ammonium bicarbonate by centrifugation at 12,000 g for 10 min. The flow-through fractions were collected and lyophilized.

The lyophilized peptides were re-suspended in ddH_2O containing 0.1% formic acid, and 2 µl aliquots of which were loaded into a nanoViper C18 (Acclaim PepMap 100, 75 µm×2 cm) trap column. The online Chromatography separation was performed on the Easy nLC 1200 system (Thermo Fisher). The trapping and desalting procedures were carried out with a volume of 20 µl 100% solvent A (0.1% formic acid). Then, an elution gradient of 5% -38% solvent B (80% acetonitrile, 0.1% formic acid) in 60 min was used on an analytical column (Acclaim PepMap RSLC, 75µm × 25cm C18-2µm 100Å). TimsTof Pro2 mass spectrometer (Bruker, USA) fitted with a Bruker captive spray ion source was operated in DIA-PASEF mode with a scan range of 100-1700 m/z and 10 PASEF ramps. The TIMS settings were 100ms ramp and accumulation time (100% duty cycle) and a ramp rate of 9.42Hz; this resulted in 1.8s of cycle time and setting at a 5000 absolute intensity threshold. The collision energy remained at default with a base of 1.60/K0[V s/cm2] set at 59eV and 0.60/K0[Vs/cm2] at 20eV. Active exclusion was enabled with a 0.4 min release. TIMS ranges were set initially from one range of 0.60−1.60/K0[V s/cm2] as seen in most published studies.

Verification of peptide identification

Peptide identification was verified using synthetic peptides. Peptides were synthesized by ChinaPeptides (Shanghai, China) at purity > 90% and dissolved to 10mM with DMSO. For LC-MS/MS measurements, peptides were pooled and further diluted with 0.1% FA/3% ACN to load 120 fmol/ml on the column. LC-MS/MS measurements were performed as described above. The sequences of experimental and synthetic spectra were confirmed by plotting the fragment ion mass spectra.

MHC-II-peptide binding assay *in vitro*

A competition assay based on the binding of a high-affinity biotin-labeled control peptide (Biotin-(Ahx)-(Ahx)-YAHAAHAAHAAHAAHAA) to MHC-II molecules was used to test peptide binding to MHC-II molecules. The assays were performed as detailed previously.(*42*) Briefly, the test peptides were diluted into a series of concentrations. These diluted test peptides were co-incubated with 0.1 μM biotin-labeled peptide and 50 nM purified MHC-II proteins (ProImmune, Oxford, United Kingdom) at 37°C for 24h in the presence of Octyl-β-D-glucopyranaside (Sigma-Aldrich). Then, the binding reaction was neutralized and transferred into MHC Class II (I-A/I-E) monoclonal antibody (M5/114.15.2) (Thermo Fisher) coated ELISA plates (Corning). The plates were incubated in a 4°C refrigerator overnight. Finally, diluted Europium-Streptavidin (Abcam, MA, USA) was added to each well of the ELISA plate, and the fluorescence was read using a time-resolved fluorescent plate reader (Thermo Fisher, MA, USA) with Europium settings. Each peptide was tested at eight different concentrations and in three independent experiments.

Peptides immunization and ELISpot assay

BALB/c mice were immunized subcutaneously with a pool of synthetic peptides (50 μg for each peptide) emulsified in Complete Freunds Adjuvant (Sigma-Aldrich). 10 days and 28 days post-vaccination, mice were sacrificed, and spleens were removed for ELISpot assays.

Splenocytes (500,000 cells/well) were treated with red blood cell lysis buffer and stimulated with peptides (5 μM) respectively in triplicate in ELISpot plates (Dakewe Biotech, Shenzhen, China) for 18 hr. Interferon-γ (IFN-γ) secretion was detected using capture and detection antibodies and imaged using an Elispot & FluoroSpot Reader (Mabtech, Stockholm, Sweden). OVA peptide$_{323\text{-}339}$ (ISQAVHAAHAEINEAGR) and

non-stimulated wells were used as negative controls. PMA (BioGems, NJ, USA) was used as a positive control. A 3-fold increase over baseline is used as a threshold for positive responses.

Prediction of peptide-MHC-II binding motifs

Peptide-MHC-II binding motifs, alignment and clustering of peptides were predicted using the MhcVizPipe (MVP) software tool (https://github.com/CaronLab/ MhcVizPipe). The MHC-II allele I-A^d or I-E^d were selected keeping all standard parameters.

MHC class II binding prediction

The online tools NetMHCIIpan 4.1, SMM align and NN_align in IEDB (https://www.iedb.org/) were used to predict the binding of MS-detected peptides and *H. pylori*- peptides to MHC-II alleles respectively. To test whether MS-detected proteins harbor more peptides compatible with the MHC-II binding motifs, all protein sequences of *H. pylori* strain NCTC 11637 were retrieved from UniProt database and compared the ratio between the number of peptides that are predicted to bind MHC-II alleles and the total number of 13- to 17-mers at a cutoff of predicted percentile rank values (%) < 2.

Statistical Analysis

Data are shown as mean ± SD. A one-way analysis of variance was performed to compare the statistical significance among 3 groups or more. Student's *t-test* was used to compare the differences between 2 groups, but when the variances differed, the Mann-Whitney test was used. The chi-square test was used to analyze differences in constituent ratios between 2 groups. Pearson's correlation was conducted to test the correlation between 2 continuous variables, and Spearman's correlation was conducted for categorical variables. SPSS statistical software (version 25; SPSS Inc, IL, USA) and GraphPad Prism (version

9.0; GraphPad Software, CA, USA) were used for statistical analysis. $P < 0.05$ was considered statistically significant.

References

1. B. Levast *et al.*, Vaccine Potentiation by Combination Adjuvants. *Vaccines (Basel)* **2**, 297-322 (2014).
2. N. Petrovsky, Comparative Safety of Vaccine Adjuvants: A Summary of Current Evidence and Future Needs. *Drug Saf* **38**, 1059-1074 (2015).
3. A. J. Sant *et al.*, The relationship between immunodominance, DM editing, and the kinetic stability of MHC class II:peptide complexes. *Immunol Rev* **207**, 261-278 (2005).
4. B. Pulendran, Modulating vaccine responses with dendritic cells and Toll-like receptors. *Immunol Rev* **199**, 227-250 (2004).
5. P. Malfertheiner *et al.*, Helicobacter pylori infection. *Nat Rev Dis Primers* **9**, 19 (2023).
6. S. F. Moss, S. C. Shah, M. C. Tan, H. B. El-Serag, Evolving Concepts in Helicobacter pylori Management. *Gastroenterology*, (2023).
7. V. Friedrich, M. Gerhard, Vaccination against Helicobacter pylori - An approach for cancer prevention? *Mol Aspects Med* **92**, 101183 (2023).
8. Q. Li *et al.*, Built-in adjuvants for use in vaccines. *Eur J Med Chem* **227**, 113917 (2022).
9. J. K. Tom *et al.*, Applications of Immunomodulatory Immune Synergies to Adjuvant Discovery and Vaccine Development. *Trends Biotechnol* **37**, 373-388 (2019).
10. A. M. Didierlaurent *et al.*, Adjuvant system AS01: helping to overcome the challenges of modern vaccines. *Expert Rev Vaccines* **16**, 55-63 (2017).
11. J. Fan *et al.*, Advances in Infectious Disease Vaccine Adjuvants. *Vaccines (Basel)* **10**, (2022).
12. G. Del Giudice, R. Rappuoli, A. M. Didierlaurent, Correlates of adjuvanticity: A review on

adjuvants in licensed vaccines. *Semin Immunol* **39**, 14-21 (2018).

13. E. Iwicka, J. Hajtuch, K. Dzierzbicka, I. Inkielewicz-Stepniak, Muramyl dipeptide-based analogs as potential anticancer compounds: Strategies to improve selectivity, biocompatibility, and efficiency. *Front Oncol* **12**, 970967 (2022).
14. C. K. Baumgartner, A. Ferrante, M. Nagaoka, J. Gorski, L. P. Malherbe, Peptide-MHC class II complex stability governs CD4 T cell clonal selection. *J Immunol* **184**, 573-581 (2010).
15. D. H. Busch, E. G. Pamer, T cell affinity maturation by selective expansion during infection. *J Exp Med* **189**, 701-710 (1999).
16. B. Li *et al.*, The influence of adjuvant on UreB protection against Helicobacter pylori through the diversity of CD4+ T-cell epitope repertoire. *Oncotarget* **8**, 68138-68152 (2017).
17. C. L. Vanderlugt, S. D. Miller, Epitope spreading in immune-mediated diseases: implications for immunotherapy. *Nat Rev Immunol* **2**, 85-95 (2002).
18. I. R. Mackay, M. J. Rowley, Autoimmune epitopes: autoepitopes. *Autoimmun Rev* **3**, 487-492 (2004).
19. J. D. Ooi *et al.*, Dominant protection from HLA-linked autoimmunity by antigen-specific regulatory T cells. *Nature* **545**, 243-247 (2017).
20. D. Maeda *et al.*, Adjuvant-Mediated Epitope Specificity and Enhanced Neutralizing Activity of Antibodies Targeting Dengue Virus Envelope Protein. *Front Immunol* **8**, 1175 (2017).
21. F. Borriello *et al.*, An adjuvant strategy enabled by modulation of the physical properties of microbial ligands expands antigen immunogenicity. *Cell* **185**, 614-629 e621 (2022).
22. K. Y. Chung *et al.*, ISCOMATRIX adjuvant promotes epitope spreading and antibody affinity maturation of influenza A H7N9 virus like particle vaccine that correlate with

virus neutralization in humans. *Vaccine* **33**, 3953-3962 (2015).

23. R. Lo-Man *et al.*, Extending the CD4(+) T-cell epitope specificity of the Th1 immune response to an antigen using a Salmonella enterica serovar typhimurium delivery vehicle. *Infect Immun* **68**, 3079-3089 (2000).

24. T. Bennekov *et al.*, Alteration of epitope recognition pattern in Ag85B and ESAT-6 has a profound influence on vaccine-induced protection against Mycobacterium tuberculosis. *Eur J Immunol* **36**, 3346-3355 (2006).

25. S. Yang, J. W. Hodge, D. W. Grosenbach, J. Schlom, Vaccines with enhanced costimulation maintain high avidity memory CTL. *J Immunol* **175**, 3715-3723 (2005).

26. J. W. Hodge, M. Chakraborty, C. Kudo-Saito, C. T. Garnett, J. Schlom, Multiple costimulatory modalities enhance CTL avidity. *J Immunol* **174**, 5994-6004 (2005).

27. L. Santambrogio, Molecular Determinants Regulating the Plasticity of the MHC Class II Immunopeptidome. *Front Immunol* **13**, 878271 (2022).

28. L. Malherbe, L. Mark, N. Fazilleau, L. J. McHeyzer-Williams, M. G. McHeyzer-Williams, Vaccine adjuvants alter TCR-based selection thresholds. *Immunity* **28**, 698-709 (2008).

29. T. T. Spear, B. D. Evavold, B. M. Baker, M. I. Nishimura, Understanding TCR affinity, antigen specificity, and cross-reactivity to improve TCR gene-modified T cells for cancer immunotherapy. *Cancer Immunol Immunother* **68**, 1881-1889 (2019).

30. N. S. Lima *et al.*, CTL Clonotypes with Higher TCR Affinity Have Better Ability to Reduce the HIV Latent Reservoir. *J Immunol* **205**, 699-707 (2020).

31. T. Burster *et al.*, Differential processing of autoantigens in lysosomes from human monocyte-derived and peripheral blood dendritic cells. *J Immunol* **175**, 5940-5949 (2005).

32. C. Stoeckle *et al.*, Cathepsin G is differentially expressed in primary human antigen-presenting cells. *Cell Immunol* **255**, 41-45 (2009).

33. X. Chen, L. M. Reed-Loisel, L. Karlsson, P. E. Jensen, H2-O expression in primary

dendritic cells. *J Immunol* **176**, 3548-3556 (2006).

34. L. Vidard, K. L. Rock, B. Benacerraf, Heterogeneity in antigen processing by different types of antigen-presenting cells. Effect of cell culture on antigen processing ability. *J Immunol* **149**, 1905-1911 (1992).

35. T. van den Hoorn, J. Neefjes, Activated pDCs: open to new antigen-presentation possibilities. *Nat Immunol* **9**, 1208-1210 (2008).

36. L. Gapin *et al.*, Antigen presentation by dendritic cells focuses T cell responses against immunodominant peptides: studies in the hen egg-white lysozyme (HEL) model. *J Immunol* **160**, 1555-1564 (1998).

37. M. Schnurr *et al.*, Tumor antigen processing and presentation depend critically on dendritic cell type and the mode of antigen delivery. *Blood* **105**, 2465-2472 (2005).

38. S. Weingarten-Gabbay *et al.*, Profiling SARS-CoV-2 HLA-I peptidome reveals T cell epitopes from out-of-frame ORFs. *Cell* **184**, 3962-3980 e3917 (2021).

39. E. Fiebiger *et al.*, Cytokines regulate proteolysis in major histocompatibility complex class II-dependent antigen presentation by dendritic cells. *J Exp Med* **193**, 881-892 (2001).

40. B. Li *et al.*, Immunodominant epitope-specific Th1 but not Th17 responses mediate protection against Helicobacter pylori infection following UreB vaccination of BALB/c mice. *Sci Rep* **5**, 14793 (2015).

41. I. Sirois, M. Isabelle, J. D. Duquette, F. Saab, E. Caron, Immunopeptidomics: Isolation of Mouse and Human MHC Class I- and II-Associated Peptides for Mass Spectrometry Analysis. *J Vis Exp*, (2021).

42. R. Salvat, L. Moise, C. Bailey-Kellogg, K. E. Griswold, A high throughput MHC II binding assay for quantitative analysis of peptide epitopes. *J Vis Exp*, (2014).

Acknowledgments

We acknowledge Miss Yunyun Shi for her help during the analysis of the proteome and peptidome data.

Funding: This study was supported by the National Nature Science Foundation of China (No. 82001751) and the Futian Healthcare Research Project (No. FTWS2021061; No. FTWS2022063).

Author contributions:

Bin Li: Funding acquisition; Project administration; Investigation; Formal analysis; draft manuscript; Writing-review and editing.

Jin Zhang: Investigation; data analysis; Methodology; Writing-review and editing.

Taojun He: Data curation; Investigation; Methodology.

Hanmei Yuan: Methodology.

Hui Wu: Methodology.

Peng Wang: Project administration; Supervision; Validation; Resources; Writing-review and editing.

Chao Wu: Conceptualization; Funding acquisition; Project administration; Supervision; Validation; Resources; Writing-review and editing.

Competing interests: The authors declare no competing interests.

Data and materials availability: All data needed to evaluate the conclusions in the paper are present in the paper and/or the Supplementary Materials. The original mass spectra and peptide spectrum matches used in this study have been deposited in the public proteomics repository iProX (https://www.iprox.cn/page/home.html) under accession number IPX0007611000. Data are also available from the corresponding authors on reasonable request.

Figure legend

Fig. 1. Immunodominant T cell epitopes in different adjuvants vaccination mice.

Spleens were collected from mice on day 10 post vaccination with antigen UreB incorporated with adjuvants CpG, MDP and MPLA respectively. Then, these cells were cultured *in vitro* and stimulated with a panel of overlapping UreB 18mer peptides to assess the responsiveness of $CD4^+$ T cells by ICS for IFN-γ. The percentages of $CD4^+$ T cells secreting IFN-γ against each peptide were determined by flow cytometry and shown. Locations of dominant peptides in different groups are indicated.

Fig. 2. MHC-II peptidome and proteome measurements in adjuvants treated APCs. A20 cells were treated with CpG, MDP and MPLA incorporated with *H. pylori* antigens for 12h, respectively. Then, most of the cells (10^8) were lysed for immunopeptidomics, and the remaining cells (10^7) were used for proteomics. **(A)** Flow chart of the experiment. **(B)** The number of MHC peptides identified in different adjuvants treated groups. n=3. Numbers indicate the Mean value. **(C)** Length distribution of MHC peptides in different adjuvants treated groups. **(D)** Sequence motifs of MHC peptides identified in adjuvants treated groups. **(E)** Binding heatmaps of all eluted MHC peptides between 9-22mers in adjuvants-treated groups were predicted and assigned to alleles using NetMHCIIpan. ns: no significant difference (P>0.05).

Fig. 3. Profiling exogenous MHC-II peptides in adjuvants treated APCs.

(A) Peptide locations across the *H. pylori* genome from MHC-II immunopeptidomes. **(B)** Rank plot of each protein abundance detected in the whole proteome of bacterial ultrasonic supernatant antigens. Proteins identified in immunopeptidomes are annotated

with their respective gene names. **(C)** MHC-II presentation potential of bacterial proteins. All reported *H. pylori* proteins were ranked according to the ratio between the number of peptides predicted to be presented by MHC-II alleles (rank≤2) and the total number of 13- to 17-mers. Proteins identified in immunopeptidomes are annotated with their respective gene names. **(D)** Heatmap of exogenous MHC peptides from different adjuvant groups. The identified sequences are shown. **(E)** Numbers of MHC peptides derived from bacteria and host were compared among different adjuvant groups. n=3. $^{**}p < 0.01$, $^{****}P < 0.0001$.

Fig. 4. Antigen phagocytosis of APCs treated with different adjuvants.

(A) Comparison of bacterial protein abundance in APCs 12h post adjuvants stimulation from whole proteomes. **(B)** Abundances of bacterial proteins from immunopeptidome and proteome were compared among adjuvant groups. $^{*}p < 0.05$, $^{**}p < 0.01$, $^{***}p < 0.001$, $^{****}P < 0.0001$.

Fig. 5. The effects of adjuvants on antigen presentation.

(A) Rank plot of protein abundances from host and bacteria in the whole-proteome of different adjuvant groups. Bacterial proteins are marked with red, and some of them are annotated with their respective gene names. **(B)** Similar to **(A)** but for MHC peptide abundances from immunopeptidomes of different adjuvant groups. Bacterial MHC peptides are annotated with their respective amino acid sequence. **(C)** Volcano plots comparing protein levels between PBS and adjuvants-treated groups in the whole-proteome. Proteins involved in antigen processing, ubiquitination, proteasome & peptidase, and IFN pathways are colored accordingly. Above the dashed line (*p-value* < 0.01) means significant.

Fig. 6. Binding affinity of MS-detected peptides were determined.

(A) IC50 values of the presented and deficient peptides post adjuvants stimulation from immunopeptidome binding to H2-IA and H2-IE were predicted by the NN align method using the IEDB website. A high IC50 value means a low binding stability. **(B)** Distribution of proteins corresponding to bacterial MHC peptides from immunopeptidome. The numbers of peptides identified by MS for each protein are indicated. **(C)** Information of 10 synthetic peptides from Top4 presented and deficient proteins. ×: Presence of peptides in the corresponding group. -: Peptides missing in the corresponding group. (**D)** Mirror plots with fragment ion mass spectra to confirm the sequences of MHC peptides from immunopeptidome. Positive y-axis, MHC-II IP sequences; negative y-axis, synthetic peptides. **(E)** Competitive binding curve of synthetic peptides for MHC II H2-IA allele. The binding curves of peptides presented in adjuvant groups are marked with red.

Fig. 7. T cell responses induced by MS-detected peptides with different binding stability were analyzed.

Five BALB/c mice were immunized with a pool of 10 synthetic peptides. On day 10 and day 28 post immunization, splenocytes were isolated and stimulated with individual peptides for IFN-γ Elisopt assay. **(A)** Flow chart of the experiment. **(B)** and **(C)** Elispot results on day 10 and day 28. OVA peptide and non-stimulated wells were used as a negative control. PMA stimulation was used as a positive control. Responses against peptides presented in adjuvant groups are marked with red. The dashed line is the 3× median of the OVA peptide used as the threshold for positive responses. The box shows the quartiles, the bar indicates median, and the whiskers show the distribution. Elispot images of positive responses from one of the immunized mice are shown. Numbers indicate the spot counts. **(D)** Epitope-specific $CD4^+$ T cells from spleens of immunized

mice were expanded *in vitro* and the IFN-γ producing $CD4^+$ T cells were assessed using the peptides pool (left). Then, the presented peptide recA#23 and the deficient peptides ureA#2 and ureA#3 post adjuvant treatment were titrated to restimulate the expanded cells (right). IFN-γ responses of $CD4^+$ T cells were detected by FACS. The responses induced by the indicated peptides at 50μM were considered as 100%. And all the other responses were evaluated by their relative strength.

Figure1

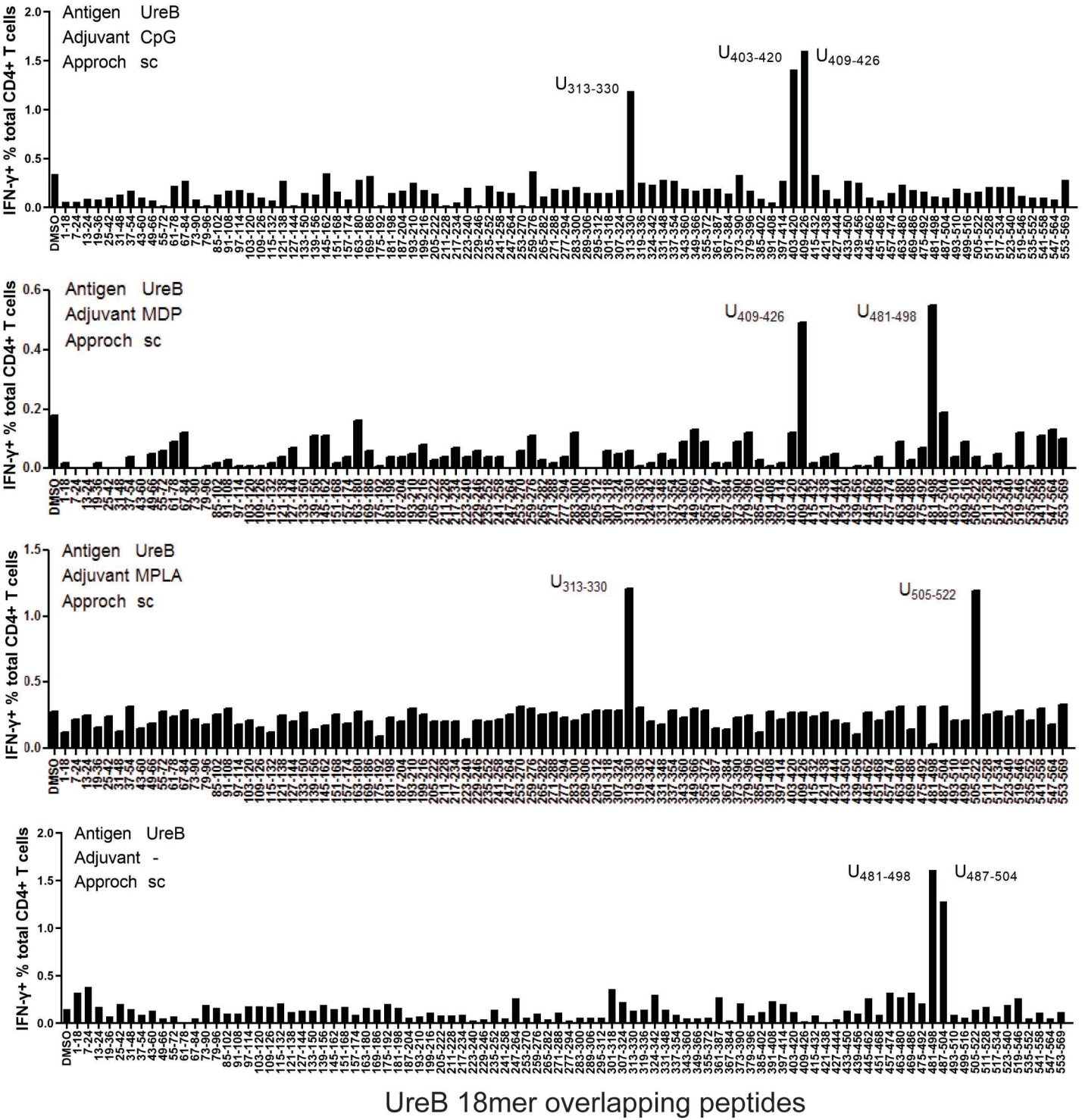
Antigen UreB
Adjuvant CpG
Approch sc
U313-330
U403-420
U409-426
Antigen UreB
Adjuvant MDP
Approch sc
U409-426
U481-498
Antigen UreB
Adjuvant MPLA
Approch sc
U313-330
U505-522
Antigen UreB
Adjuvant -
Approch sc
U481-498
U487-504
IFN-γ+ % total CD4+ T cells
UreB 18mer overlapping peptides

Figure2

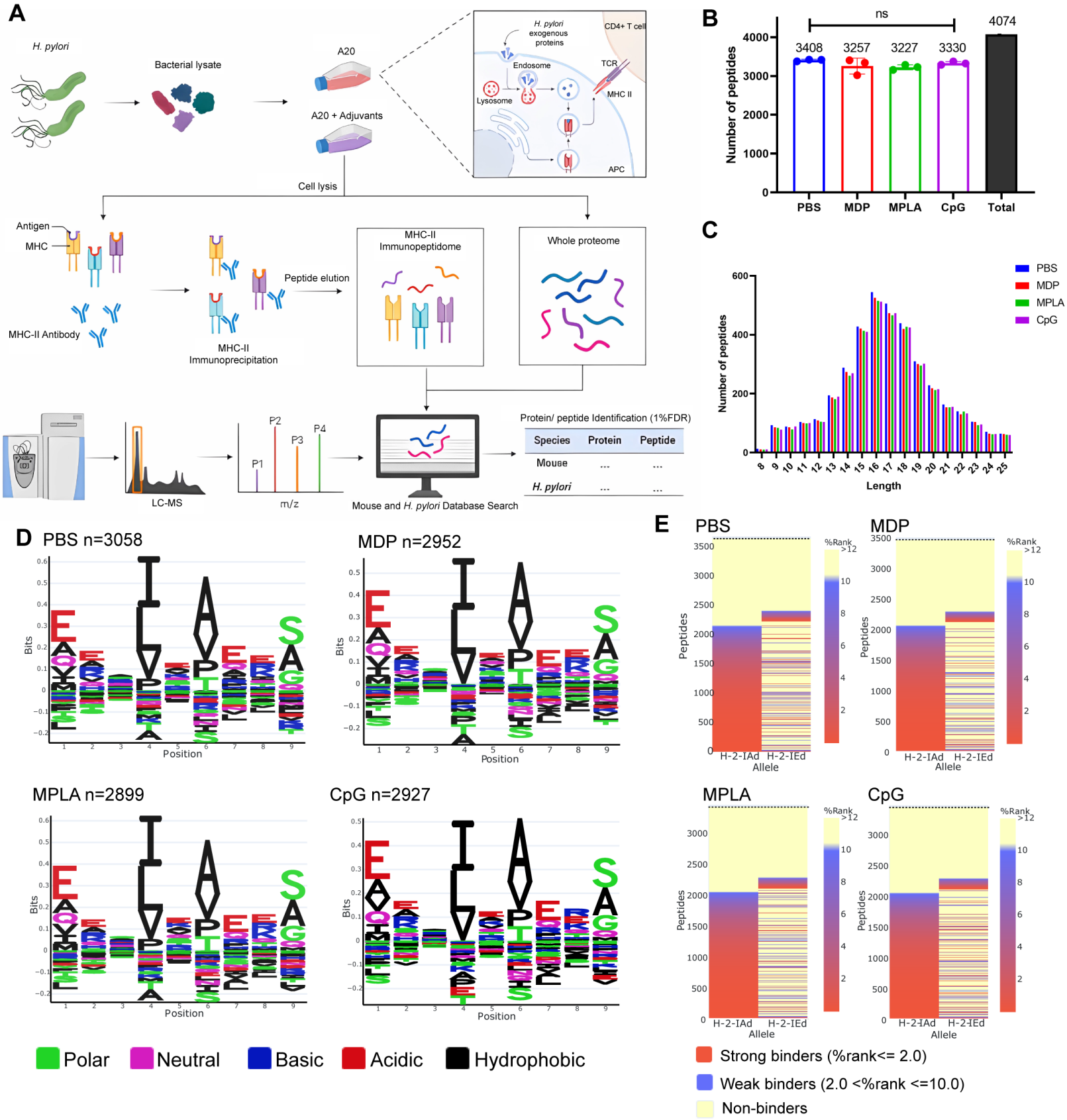
A
H. pylori
Bacterial lysate
A20
A20 + Adjuvants
Cell lysis
H. pylori exogenous proteins
CD4+ T cell
Endosome
Lysosome
TCR
MHC II
APC
Antigen
MHC
MHC-II Antibody
MHC-II Immunoprecipitation
Peptide elution
MHC-II Immunopeptidome
Whole proteome
LC-MS
P1
P2
P3
P4
m/z
Mouse and H. pylori Database Search
Protein/ peptide Identification (1%FDR)
Species
Protein
Peptide
Mouse
H. pylori
B
ns
Number of peptides
3408
3257
3227
3330
4074
PBS
MDP
MPLA
CpG
Total
C
PBS
MDP
MPLA
CpG
Number of peptides
Length
D
PBS n=3058
MDP n=2952
MPLA n=2899
CpG n=2927
Bits
Position
Polar
Neutral
Basic
Acidic
Hydrophobic
E
PBS
MDP
MPLA
CpG
Peptides
Allele
H-2-IAd
H-2-IEd
%Rank
Strong binders (%rank<= 2.0)
Weak binders (2.0 <%rank <=10.0)
Non-binders

Figure3

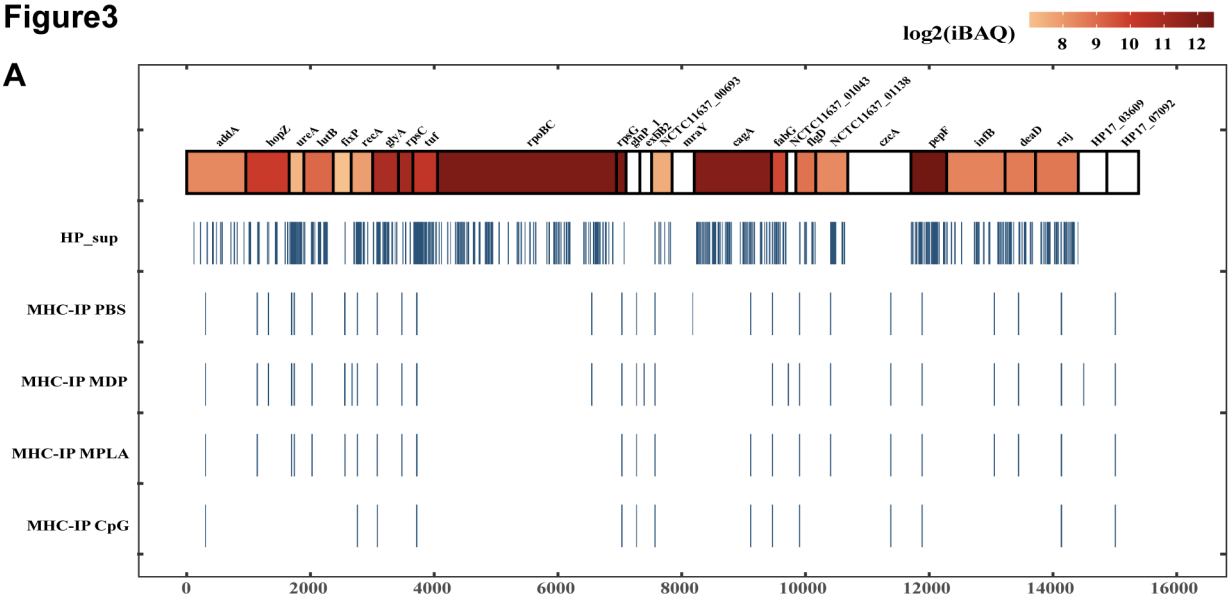
log2(iBAQ)
8 9 10 11 12
A
addA
hopZ
ureA
lutB
fixP
recA
glyA
rpsC
tuf
rpoBC
rpsG
glnP_1
exbB2
NCTC11637_00693
mraY
cagA
fabG
NCTC11637_01043
flgD
NCTC11637_01138
czcA
pepF
infB
deaD
rnj
HP17_03609
HP17_07092
HP_sup
MHC-IP PBS
MHC-IP MDP
MHC-IP MPLA
MHC-IP CpG
0
2000
4000
6000
8000
10000
12000
14000
16000

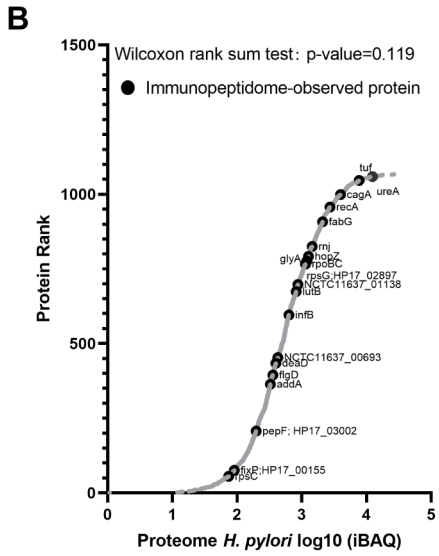
B
Wilcoxon rank sum test: p-value=0.119
Immunopeptidome-observed protein
Protein Rank
Proteome H. pylori log10 (iBAQ)
tuf
ureA
cagA
recA
fabG
rnj
glyA
hopZ
rpoBC
rpsG:HP17_02897
NCTC11637_01138
lutB
infB
NCTC11637_00693
deaD
flgD
addA
pepF: HP17_03002
fixP:HP17_00155
rpsC

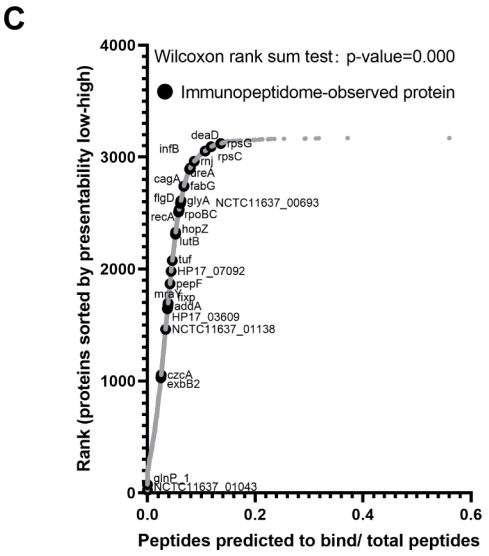
C
Wilcoxon rank sum test: p-value=0.000
Immunopeptidome-observed protein
Rank (proteins sorted by presentability low-high)
Peptides predicted to bind/ total peptides
deaD
rpsG
infB
rnj
rpsC
ureA
cagA
fabG
flgD
glyA
NCTC11637_00693
recA
rpoBC
hopZ
lutB
tuf
HP17_07092
pepF
mra
fixp
addA
HP17_03609
NCTC11637_01138
czcA
exbB2
glnP_1
NCTC11637_01043

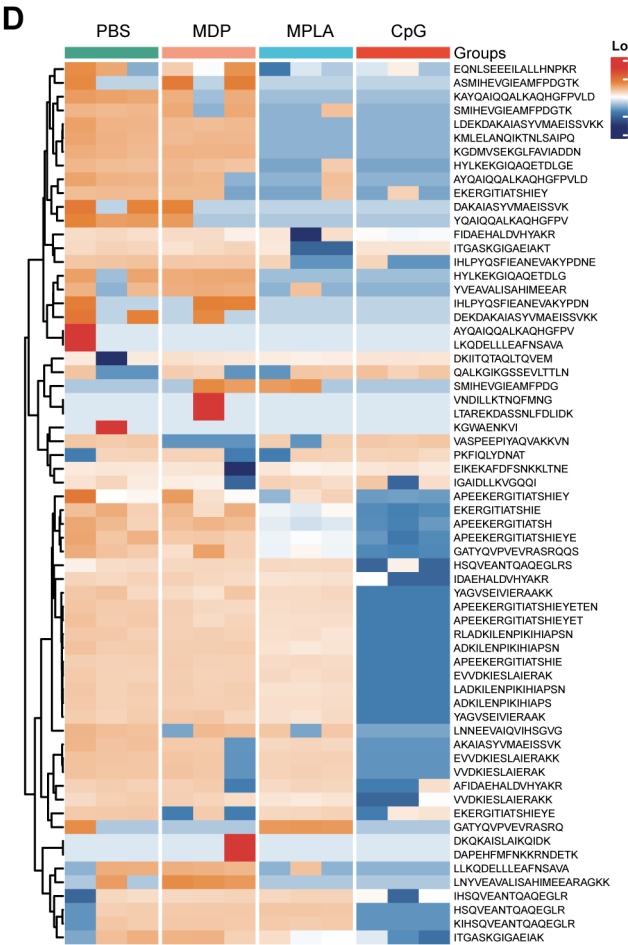
D
PBS
MDP
MPLA
CpG
Groups
Log10(iBAQ+1)
EQNLSEEEILALLHNPKR
ASMIHEVGIEAMFPDGTK
KAYQAIQQALKAQHGFPVLD
SMIHEVGIEAMFPDGTK
LDEKDAKAIASYVMAEISSVKK
KMLELANQIKTNLSAIPQ
KGDMVSEKGLFAVIADDN
HYLKEKGIQAQETDLGE
AYQAIQQALKAQHGFPVLD
EKERGITIATSHIEY
DAKAIASYVMAEISSVK
YQAIQQALKAQHGFPV
FIDAEHALDVHYAKR
ITGASKGIGAEIAKT
IHLPYQSFIEANEVAKYPDNE
HYLKEKGIQAQETDLG
YVEAVALISAHIMEEAR
IHLPYQSFIEANEVAKYPDN
DEKDAKAIASYVMAEISSVKK
AYQAIQQALKAQHGFPV
LKQDELLLEAFNSAVA
DKIITQTAQLTQVEM
QALKGIKGSSEVLTTLN
SMIHEVGIEAMFPDG
VNDILLKTNQFMNG
LTAREKDASSNLFDLIDK
KGVAENKVI
VASPEEPIYAQVAKKVN
PKFIQLYDNAT
EIKEKAFDFSNKKLTNE
IGAIDLLKVGQQI
APEEKERGITIATSHIEY
EKERGITIATSHIE
APEEKERGITIATSH
APEEKERGITIATSHIEYE
GATYQVPVEVRASRQQS
HSQVEANTQAQEGLRS
IDAEHALDVHYAKR
YAGVSEIVIERAAKK
APEEKERGITIATSHIEYETEN
APEEKERGITIATSHIEYET
RLADKILENPIKIHIAPSN
ADKILENPIKIHIAPSN
APEEKERGITIATSHIE
EVVDKIESLAIERAK
LADKILENPIKIHIAPSN
ADKILENPIKIHIAPS
YAGVSEIVIERAAK
LNNEEVAIQVIHSGVG
AKAIASYVMAEISSVK
EVVDKIESLAIERAKK
VVDKIESLAIERAK
AFIDAEHALDVHYAKR
VVDKIESLAIERAKK
EKERGITIATSHIEYE
GATYQVPVEVRASRQ
DKQKAISLAIKQIDK
DAPEHFMFNKKRNDETK
LLKQDELLLEAFNSAVA
LNYVEAVALISAHIMEEARAGKK
IHSQVEANTQAQEGLR
HSQVEANTQAQEGLR
KIHSQVEANTQAQEGLR
ITGASKGIGAEIAK

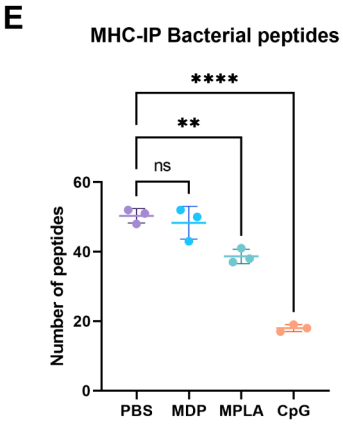
E
MHC-IP Bacterial peptides
****
**
ns
Number of peptides
PBS
MDP
MPLA
CpG

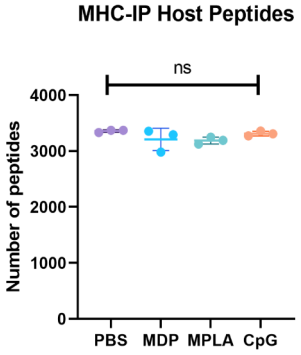
MHC-IP Host Peptides
ns
Number of peptides
PBS
MDP
MPLA
CpG

Figure4

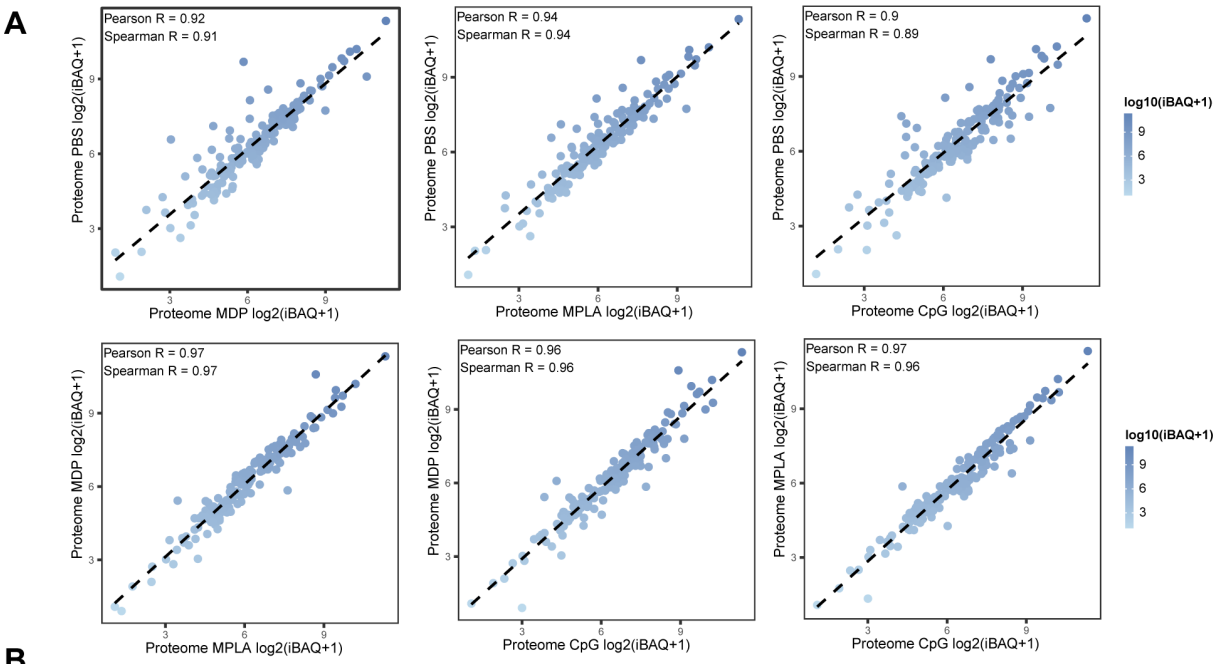
A
Pearson R = 0.92
Spearman R = 0.91
Proteome PBS log2(iBAQ+1)
Proteome MDP log2(iBAQ+1)
Pearson R = 0.94
Spearman R = 0.94
Proteome PBS log2(iBAQ+1)
Proteome MPLA log2(iBAQ+1)
Pearson R = 0.9
Spearman R = 0.89
Proteome PBS log2(iBAQ+1)
Proteome CpG log2(iBAQ+1)
log10(iBAQ+1)
Pearson R = 0.97
Spearman R = 0.97
Proteome MDP log2(iBAQ+1)
Proteome MPLA log2(iBAQ+1)
Pearson R = 0.96
Spearman R = 0.96
Proteome MDP log2(iBAQ+1)
Proteome CpG log2(iBAQ+1)
Pearson R = 0.97
Spearman R = 0.96
Proteome MPLA log2(iBAQ+1)
Proteome CpG log2(iBAQ+1)
log10(iBAQ+1)

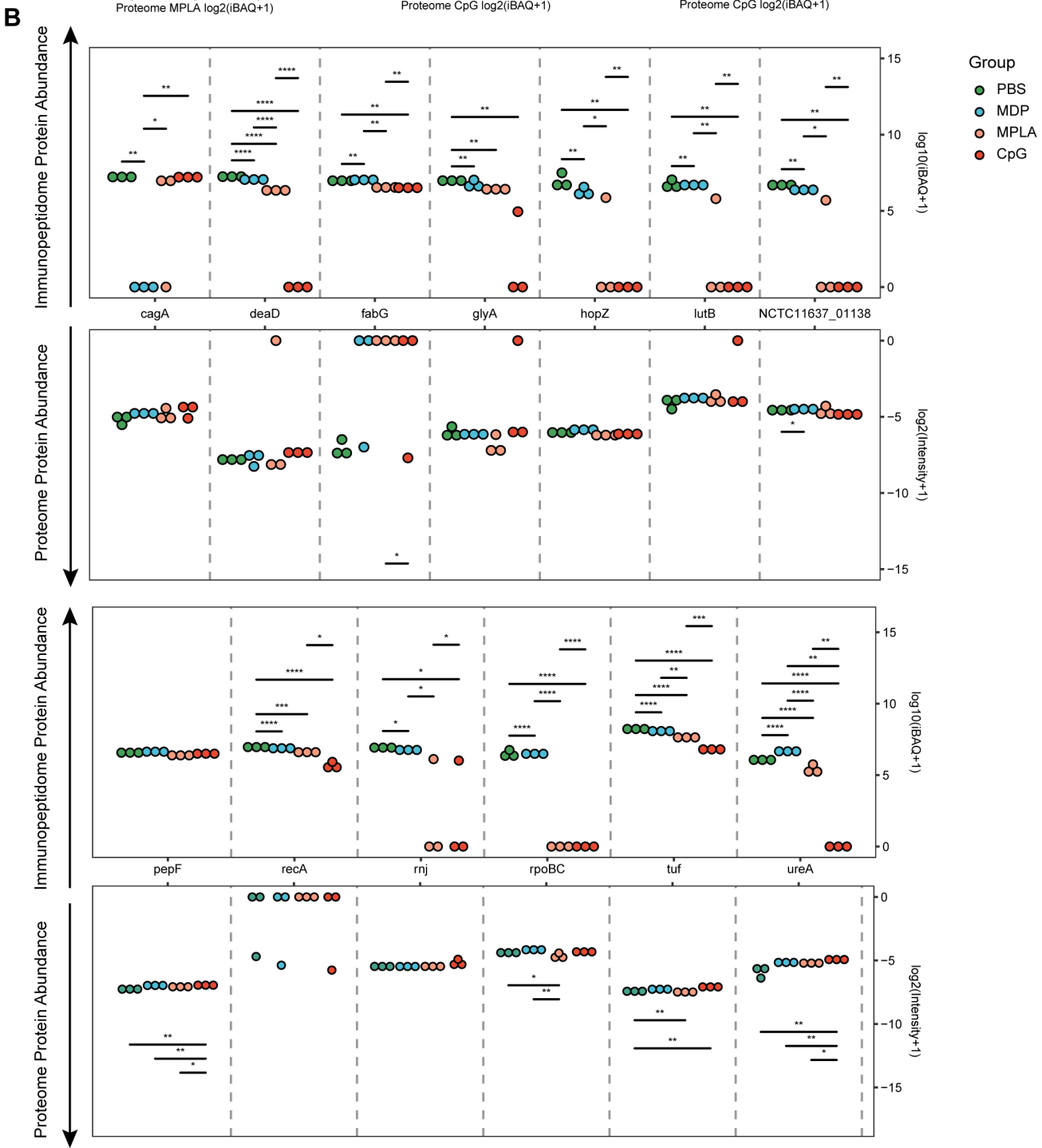
B
Immunopeptidome Protein Abundance
Proteome Protein Abundance
log10(iBAQ+1)
log2(Intensity+1)
Group
PBS
MDP
MPLA
CpG
cagA
deaD
fabG
glyA
hopZ
lutB
NCTC11637_01138
pepF
recA
rnj
rpoBC
tuf
ureA

Figure5

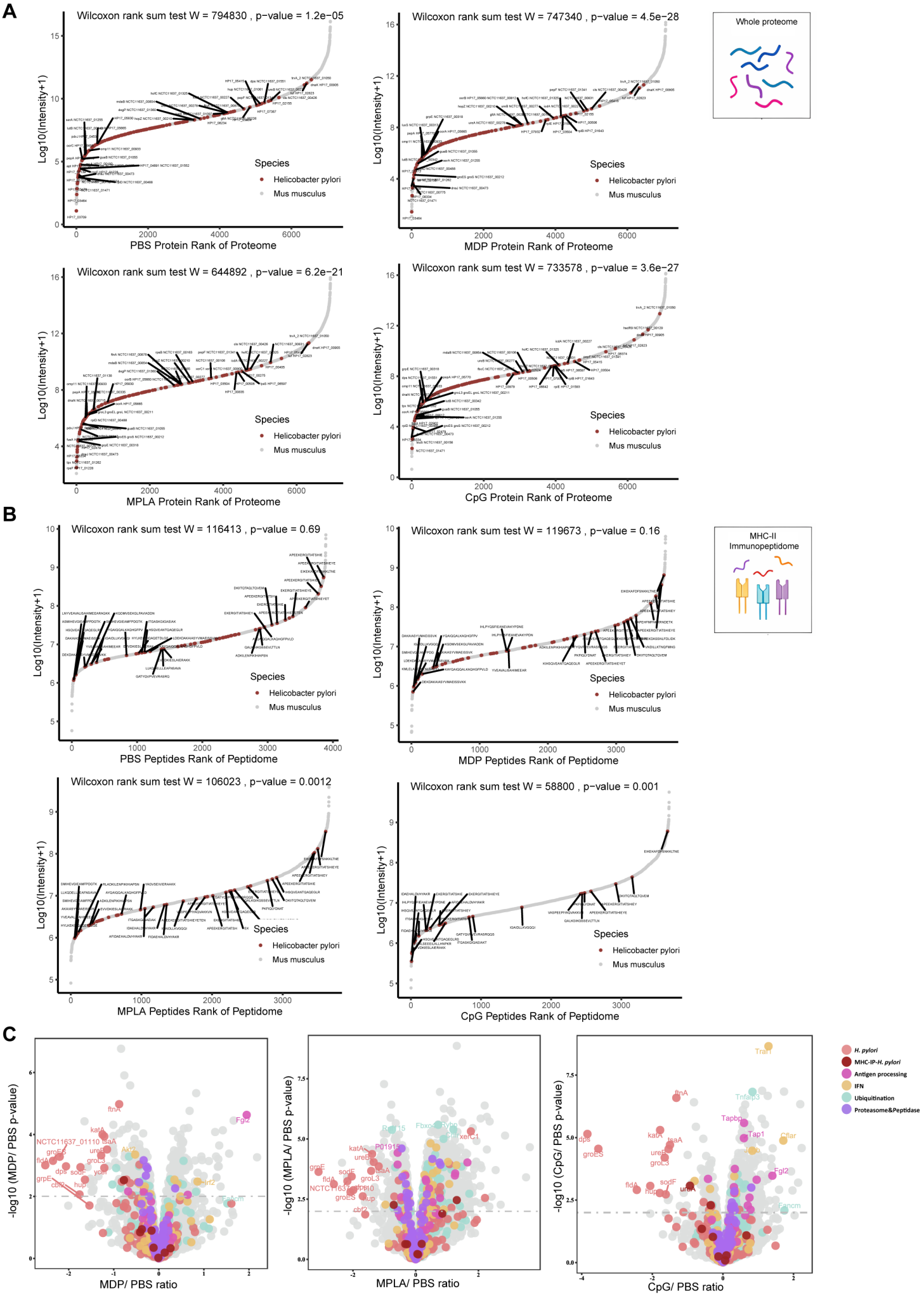
A
Wilcoxon rank sum test W = 794830 , p−value = 1.2e−05
PBS Protein Rank of Proteome
Wilcoxon rank sum test W = 747340 , p−value = 4.5e−28
MDP Protein Rank of Proteome
Wilcoxon rank sum test W = 644892 , p−value = 6.2e−21
MPLA Protein Rank of Proteome
Wilcoxon rank sum test W = 733578 , p−value = 3.6e−27
CpG Protein Rank of Proteome
Log10(Intensity+1)
Species
Helicobacter pylori
Mus musculus
Whole proteome
B
Wilcoxon rank sum test W = 116413 , p−value = 0.69
PBS Peptides Rank of Peptidome
Wilcoxon rank sum test W = 119673 , p−value = 0.16
MDP Peptides Rank of Peptidome
Wilcoxon rank sum test W = 106023 , p−value = 0.0012
MPLA Peptides Rank of Peptidome
Wilcoxon rank sum test W = 58800 , p−value = 0.001
CpG Peptides Rank of Peptidome
MHC-II Immunopeptidome
C
-log10 (MDP/ PBS p-value)
MDP/ PBS ratio
-log10 (MPLA/ PBS p-value)
MPLA/ PBS ratio
-log10 (CpG/ PBS p-value)
CpG/ PBS ratio
H. pylori
MHC-IP-H. pylori
Antigen processing
IFN
Ubiquitination
Proteasome&Peptidase

Figure6

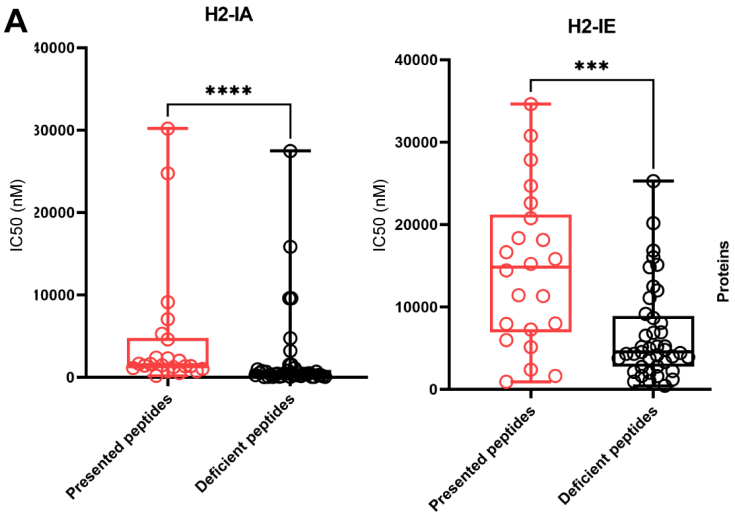

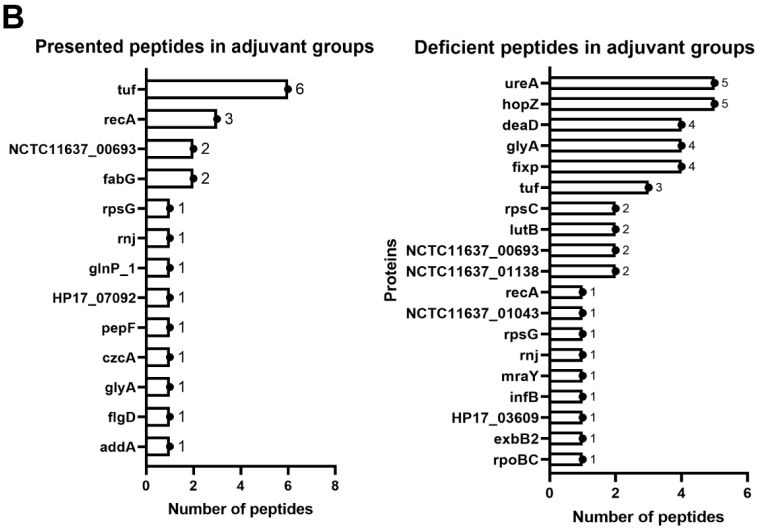

C

Name	Sequences	PBS	MDP	MPLA	CpG
ureA #2	ASMIHEVGIEAMFPDGTK	×	×	-	-
ureA #3	YVEAVALISAHIMEEAR	×	×	×	-
deaD #35	RLADKILENPIKIHIAPSN	×	×	×	-
hopZ #53	KMLELANQIKTNLSAIPQ	×	×	-	-
hopZ #55	YQAIQQALKAQHGFPV	×	×	-	-
glyA #58	EVVDKIESLAIERAKK	×	×	×	-
tuf #7	APEEKERGITIATSHIEYE	×	×	×	×
recA #23	AFIDAEHALDVHYAKR	×	×	×	×
NCTC11637_00693 #38	IHSQVEANTQAQEGLR	×	×	×	×
fabG #62	ITGASKGIGAEIAKT	×	×	×	×

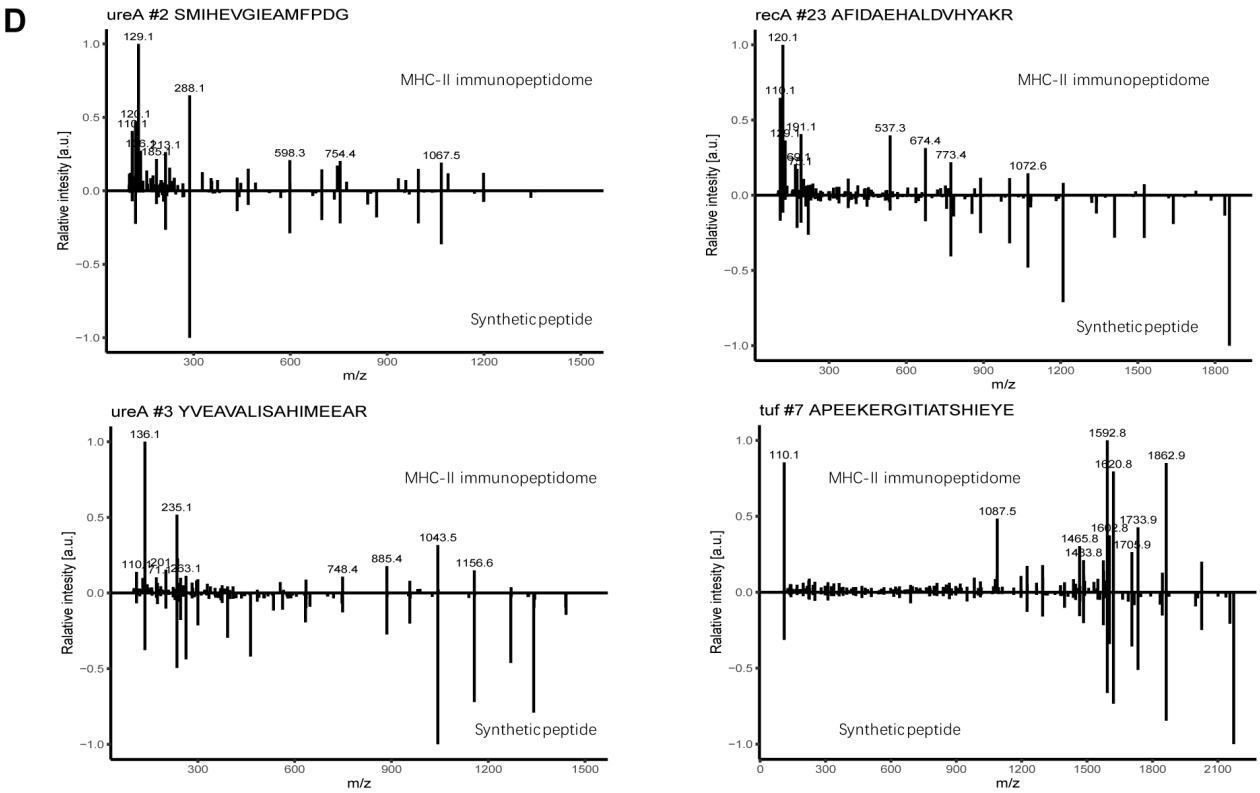

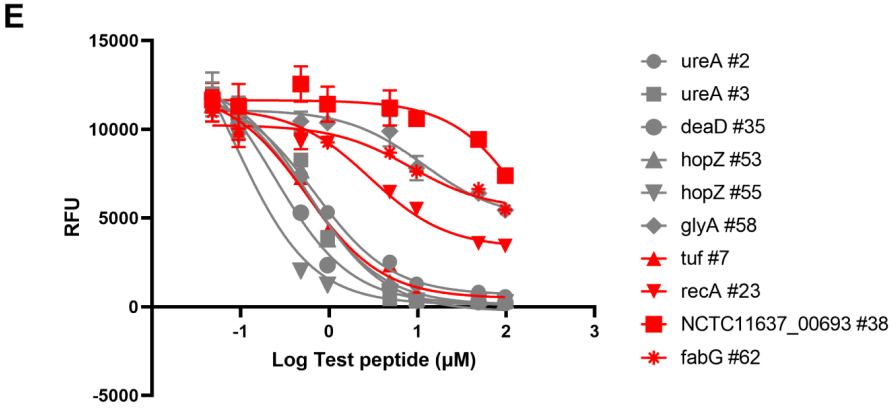

Figure7

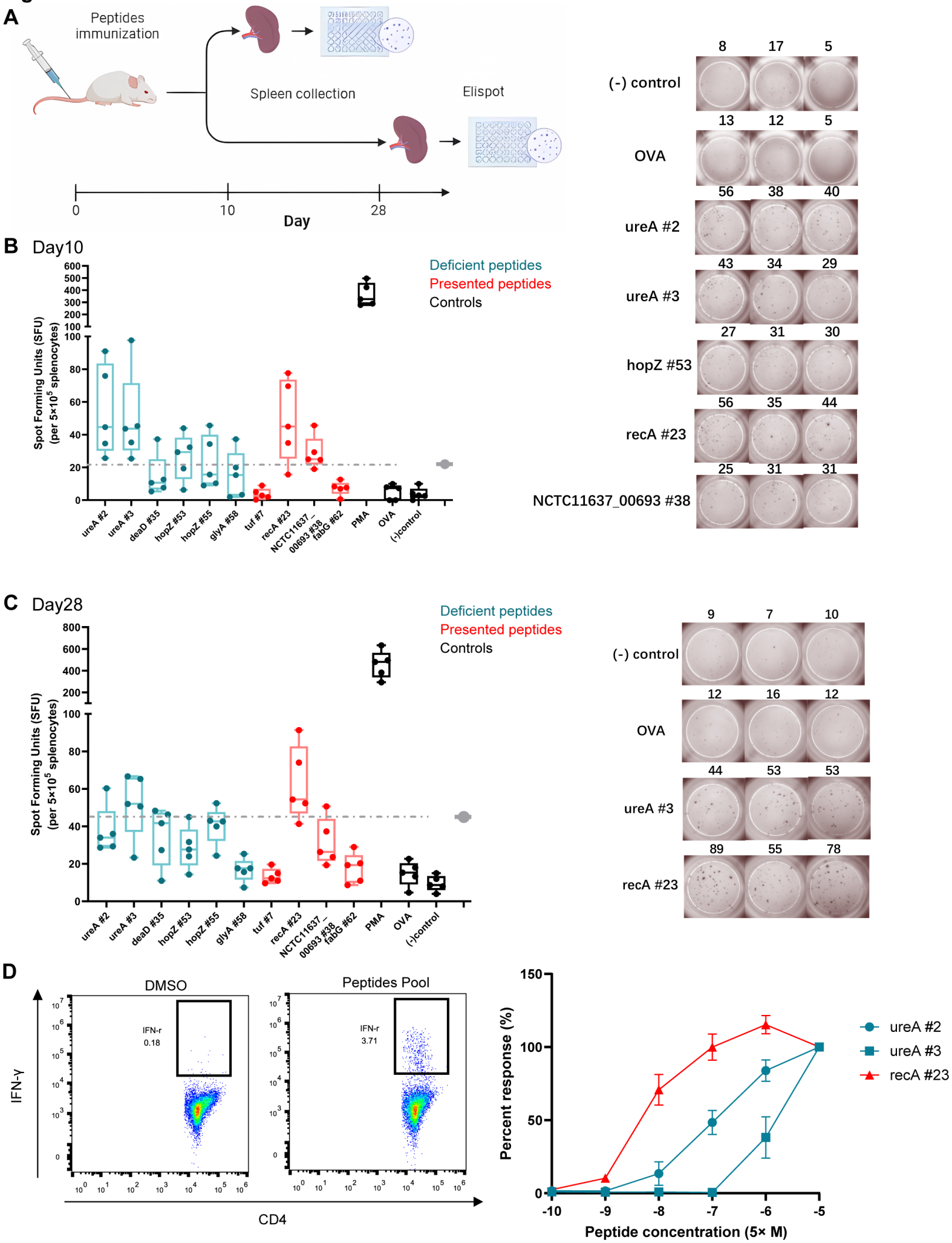
A
Peptides immunization
Spleen collection
Elispot
0
10
28
Day
(-) control
OVA
ureA #2
ureA #3
hopZ #53
recA #23
NCTC11637_00693 #38
B Day10
Deficient peptides
Presented peptides
Controls
Spot Forming Units (SFU) (per 5×10^5 splenocytes)
ureA #2
ureA #3
deaD #35
hopZ #53
hopZ #55
glyA #58
tuf #7
recA #23
NCTC11637_00693 #38
fabG #62
PMA
OVA
(-)control
C Day28
D
DMSO
Peptides Pool
IFN-r 0.18
IFN-r 3.71
IFN-γ
CD4
Percent response (%)
Peptide concentration (5× M)
ureA #2
ureA #3
recA #23